INSTITUTE OF PHYSICS PUBLISHING NANOTECHNOLOGY
Nanotechnology **17** (2006) S64–S68 doi:10.1088/0957-4484/17/4/010

Electrolysis-based diaphragm actuators

C Pang[1], Y-C Tai[1], J W Burdick[2] and R A Andersen[3]

[1] Caltech Micromachining Lab, California Institute of Technology, Pasadena, CA 91125, USA
[2] Department of Mechanical Engineering, California Institute of Technology, Pasadena, CA 91125, USA
[3] Division of Biology, California Institute of Technology, Pasadena, CA 91125, USA

E-mail: changlin@caltech.edu (C Pang)

Received 25 July 2005
Published 25 January 2006
Online at stacks.iop.org/Nano/17/S64

Abstract
This work presents a new electrolysis-based microelectromechanical systems (MEMS) diaphragm actuator. Electrolysis is a technique for converting electrical energy to pneumatic energy. Theoretically electrolysis can achieve a strain of 136 000% and is capable of generating a pressure above 200 MPa. Electrolysis actuators require modest electrical power and produce minimal heat. Due to the large volume expansion obtained via electrolysis, small actuators can create a large force. Up to 100 μm of movement was achieved by a 3 mm diaphragm. The actuator operates at room temperature and has a latching and reversing capability.

(Some figures in this article are in colour only in the electronic version)

1. Introduction

Recent studies using neural probes indicate that it is highly desirable for the probes to have the capability of moving (both forward and backward) so that they can track a specific neuron in the brain, because living neurons do move around (Andersen *et al* 2004). However, for use in the brain a movable neural probe needs to be powerful (to penetrate brain tissue) with high density, low power, bidirectionality and latchability (without power). We have since proposed the development of electrolysis-based actuators for use as movable probes. This work presents our initial work on a large-force bidirectional electrolysis actuator fabricated with microelectromechanical systems (MEMS) technology.

Electrolysis is a technique for converting electrical energy to pneumatic energy. The two electrochemical half-reactions for the electrolysis of water are shown in equations (1) and (2). The net reaction (equation (3)) entails a 3:2 stoichiometric ratio of gas to liquid and occurs via the transfer of four equivalents of electrons through an external circuit:

$$2H_2O(l) \underset{\text{recombination}}{\overset{\text{electrolysis}}{\rightleftharpoons}} O_2(g) + 4H^+(aq) + 4e^- \quad (1)$$

$$4H^+(aq) + 4e^- \underset{\text{recombination}}{\overset{\text{electrolysis}}{\rightleftharpoons}} H_2(g) \quad (2)$$

$$\text{Net: } 2H_2O(l) \underset{\text{recombination}}{\overset{\text{electrolysis}}{\rightleftharpoons}} O_2(g) + 2H_2(g). \quad (3)$$

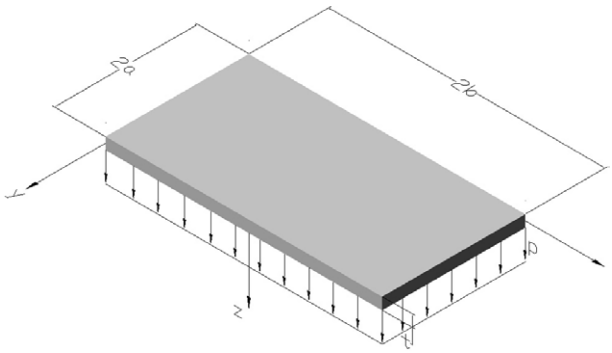

Figure 1. Geometry of a rectangular membrane.

Since an actuator device based on these reactions is powered by the gas it generates, its response will be governed approximately by the ideal gas law:

$$PV = nRT. \quad (4)$$

The maximum fractional change in length $\Delta L/L$, or strain, can be calculated by the volume change at constant pressure,

$$V_{\text{gas}} = (3/2)n_{H_2O}RT/P \quad (5)$$

$$V_{\text{liquid}} = n_{H_2O} \times M_{H_2O}/\rho_{H_2O} \quad (6)$$

where M_{H_2O} and ρ_{H_2O} are the molecular weight and density of water, respectively, and n_{H_2O} is the number of moles of

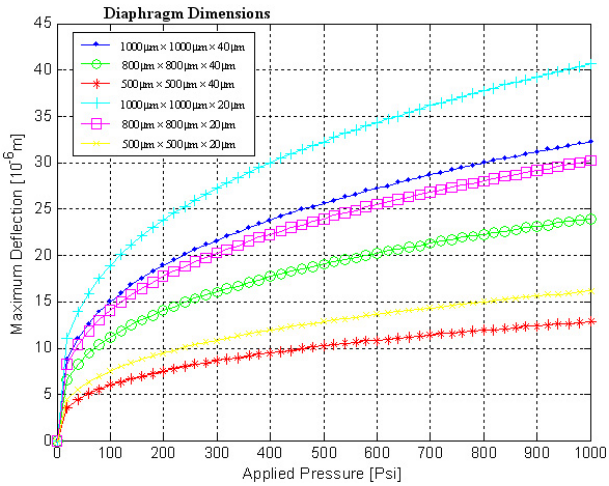

Figure 2. Theoretical displacement of a single diaphragm versus electrolysis pressure for diaphragms of various sizes.

water that are transformed. The maximum relative strain under ambient conditions can be calculated from:

$$\text{strain} = \frac{(\text{actuated length}) - (\text{unactuated length})}{\text{unactuated length}} \tag{7}$$

$$= \frac{V_{\text{gas}} - V_{\text{liquid}}}{V_{\text{liquid}}} \tag{8}$$

$$\approx \frac{V_{\text{gas}}}{V_{\text{liquid}}} \tag{9}$$

$$= \frac{(3/2)RT/P_{\text{atm}}}{M_{\text{H}_2\text{O}}/\rho_{\text{H}_2\text{O}}} \approx 136\,000\%. \tag{10}$$

The maximum stress is reached when the gas is confined to the small volume made available by the water consumed:

$$P = \frac{(3/2)n_{\text{H}_2\text{O}}RT}{V_{\text{liquid}}} \tag{11}$$

$$= \frac{(3/2)RT}{M_{\text{H}_2\text{O}}/\rho_{\text{H}_2\text{O}}} \approx 200\ \text{MPa}. \tag{12}$$

Therefore electrolysis can theoretically achieve a strain of 136 000%, and is capable of generating a pressure above 200 MPa (Cameron and Freund 2002). Electrolysis is a good method for high-performance actuation. The electrolysis pump was first demonstrated by Xie (Xie *et al* 2004). The electrolysis-based diaphragm actuators described in this paper require modest electrical power and produce minimal heat. Due to the large volume expansion obtained with electrolysis, the small actuators can create a large force. Up to 100 μm (comparable to the averaged neuron-to-neuron distance) of movement was achieved by a 3 mm diaphragm. The bidirectional movement can be linearly controlled by small currents. The actuator proved to be latchable. While electrolysis-based actuators may not extend rapidly, our preliminary results show that such speed is unnecessary. Overall the results support the promising aspects of electrolysis-based movable neural probes.

2. Simulations

The loading–deflection behaviour of a flat rectangular membrane, schematically shown in figure 1 with the two

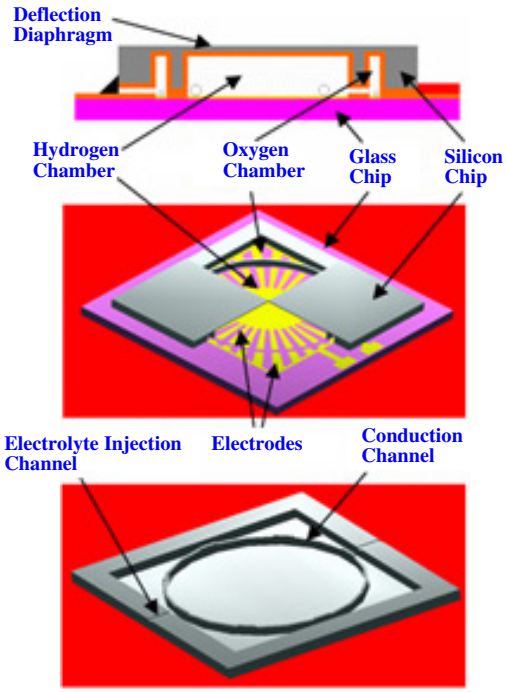

Figure 3. Schematic view of the electrolysis-based actuator.

sides $2a$ and $2b$ ($a \leqslant b$), can be described using the equations (13)–(15):

$$p = \frac{C_1 \sigma t h}{a^2} + \frac{C_2 E t h^3}{a^4} \tag{13}$$

$$C_1 = \frac{\pi^4(1+n^2)}{64} \tag{14}$$

$$C_2 = \frac{\pi^6}{32(1-\nu^2)}\left\{\frac{9+2n^2+9n^4}{256} - \left[\frac{(4+n+n^2+4n^3-3n\nu(1+n))^2}{2\{81\pi^2(1+n^2)+128n+\nu[128n-9\pi^2(1+n^2)]\}}\right]\right\} \tag{15}$$

where p is the pressure generated by electrolysis, E is the Young's modulus of the diaphragm material ($E = 170$ GPa for silicon), σ is the internal stress, t is the diaphragm thickness and h is the membrane deflection. C_1 and C_2 are constants determined by the shape of the membrane and Poisson's ratio, ν. C_1 and C_2 are 3.04 and 1.83, respectively, for a square membrane ($b/a = 1$) with an averaged Poisson's ratio of $\nu = 0.25$ for silicon.

Based on an electrolysis pressure of 300 psi (2.07×10^6 Pa), which has already been demonstrated in previous work at our laboratory, and silicon diaphragm dimensions of $1000 \times 1000 \times 40\ \mu\text{m}^3$, the maximum diaphragm deflection is $h_{\max} = 22\ \mu$m. We actually anticipate that significantly higher pressures will be realized (up to 1000 psi (6.90×10^6 Pa) using an analogous process has already been reported). With these higher pressures we can reduce the actuator size, or increase its travel. Figure 2 shows how deflection scales with electrolysis pressure for diaphragms of different sizes.

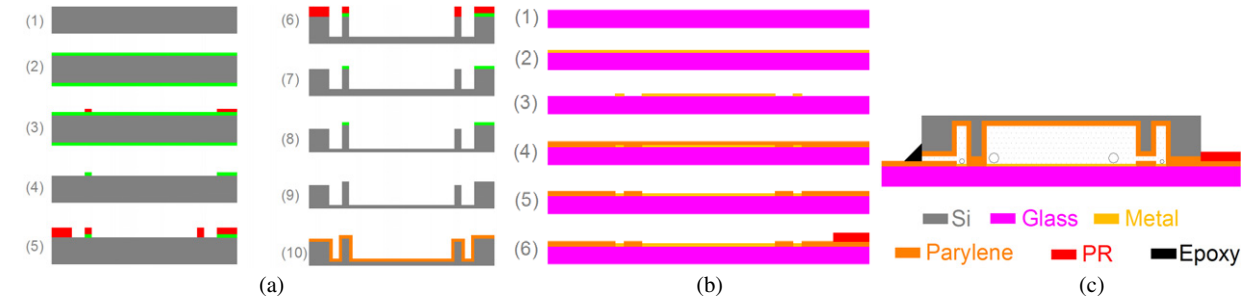

Figure 4. Fabrication process. (a) Process flow for the silicon top chip: (1) clean wafer (Piranha, 5% HF dip); (2) oxidation 1000 Å SiO_2; (3) patterning the photoresist; (4) open SiO_2 window for the entire etching area; (5) patterning a thick photoresist layer for the deep etching area; (6) DRIE etch for the chambers (∼470 μm); (7) strip photoresist; (8) DRIE etch 10 μm for the channels between the chambers and the electrolyte injection channels; (9) removal of the oxide layer; (10) coating with bonding polymer. (b) Process flow for the glass bottom chip: (1) clean wafer; (2) deposition of the metal layer (Ti/Au); (3) patterning the metal layer for the electrolysis electrodes; (4) deposition of the bonding polymer; (5) patterning the polymer layer; (6) coating and patterning the photoresist for aligning the assembly. (c) Thermally bond the two chips together.

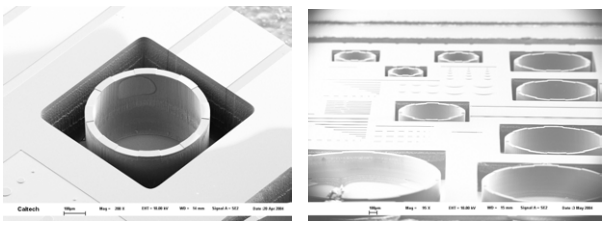

Figure 5. SEM pictures of the actuator chambers.

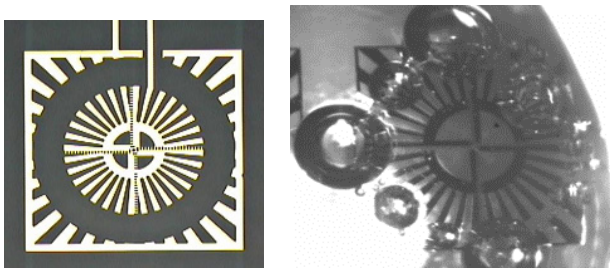

Figure 6. (a) Electrodes of the actuator. (b) Electrolysis generated by the electrodes.

3. Device design

A schematic diagram of the actuator is shown in figure 1, where two neighbouring chambers are etched in the silicon chip using deep reactive ion etching (DRIE). The central chamber is for hydrogen (generated by electrolysis) and the outside for oxygen. The chamber volume ratio is 2:1 assuming stoichiometric electrolysis. These two chambers are separated by a ring-shaped wall with a high aspect ratio. On the outside, two channels are used to fill the chambers with electrolyte. Electrolysis electrodes are made on a separate glass chip, which is later bonded to the silicon top using polymers. The central silicon membrane (with a thickness of 40 μm) deflects under the pressure generated by electrolysis. Separating oxygen and hydrogen into different chambers prevents their recombination. Therefore, the diaphragm can maintain its position even when the electrolysis is 'off'; hence it is latchable. To achieve bidirectional movement, we can reverse the polarity of the electrolysis. If the electrolysis is reversed, the newly generated gases will mix and the oxygen and hydrogen will recombine (in the presence of platinum catalyst), but only to the controlled amount defined by the reversed electrolysis.

4. Fabrication process

A two-level DRIE etching process is used to fabricate the silicon top chip (figure 4(a)). The deep etching is for the gas chambers and the shallow etching is to make the conduction and electrolyte injection channels. A variety of actuator sizes have been made, ranging from 400 to 3000 μm (figure 5). A Ti/Au layer is used for the electrode on the glass chip (figure 4(b)). Bonding polymer (either parylene or photoresist) is applied to bond the silicon top and the glass bottom chips (figure 4(c)).

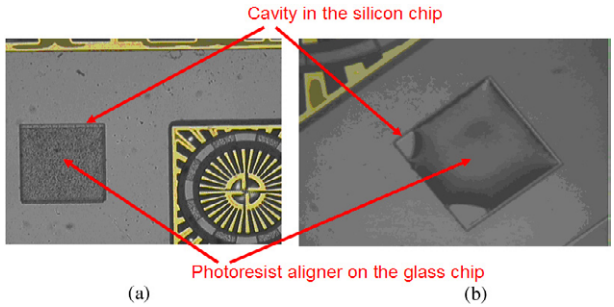

Figure 7. (a) Device aligned with the photoresist aligner. (b) The photoresist aligner reflows in the silicon cavity and sticks the two chips together. Pictures were taken from the back side of the glass electrode chip after the two chips were assembled together.

5. Fabrication results

Figure 5 shows the DRIE-fabricated silicon top chips. The central and outside chambers are etched 480 μm deep into

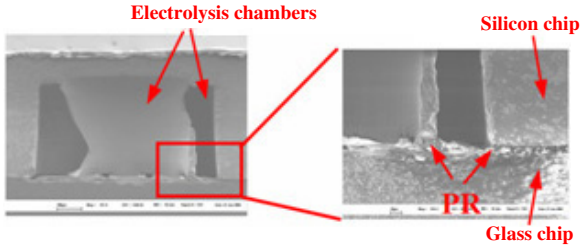

Figure 8. SEM pictures of the cross section of the photoresist-bonded device.

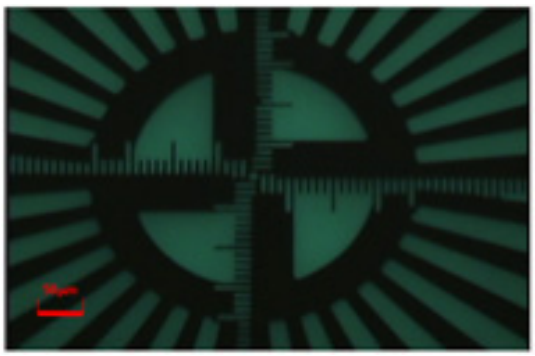

Figure 9. Fluorescent microscope image of the electrolyte-filled chamber.

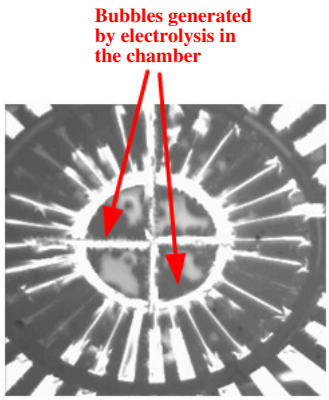

Figure 10. Electrolysis in the actuator chamber.

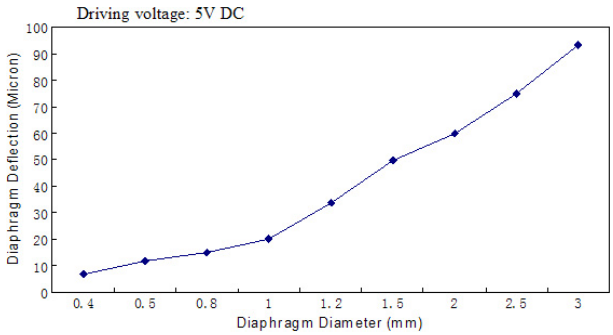

Figure 11. The deflection of different sized actuators under 5 V voltage.

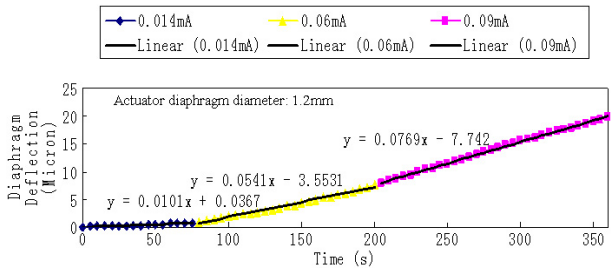

Figure 12. Diaphragm deflection under different driving currents.

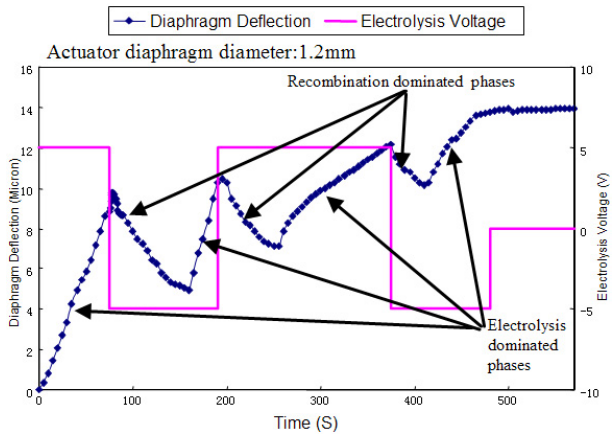

Figure 13. Testing the actuator's reversing and latching capability.

the silicon, leaving a 40 μm thick membrane at the bottom. Because of the high-aspect-ratio etching performance of DRIE, the ring-shaped separation wall is well made with a width of 50 μm and a depth of 480 μm. Ten micrometres is etched to make the conduction channels between the two chambers and the electrolyte injection channels.

Figure 6(a) shows the Ti/Au electrodes on the glass chip, with the cathode for the central hydrogen chamber and the anode for the outside oxygen chamber. Acute electrolysis (quick electrolysis testing) is well performed using the electrodes with a 3 V DC input as shown in figure 4(b).

The photoresist layer is patterned as the aligner to help in assembling the silicon chip onto the glass chip. The photoresist aligner fits into the cavity of the silicon chip (figure 7(a)), reflows at 160 °C and sticks the two chips together after it has cooled down (figure 7(b)). Finally we used thermal bonding to bond the two chips firmly and seal the chambers around the side wall, leaving only the conduction channels and electrolyte injection channels open. We tried two kinds of bonding method using either parylene or photoresist (Pan *et al* 2002). Based on the experimental data for diaphragm deflection, calculation shows that the photoresist bonding can hold under pressures as high as 500 psi (3.45×10^6 Pa). Figure 8 shows SEM pictures of the photoresist-bonded device. Photoresist has a very good sealing capability.

Filling the chambers with electrolyte is done by immersing the bonded chambers in the electrolyte under a vacuum, where the air in the chambers is first evacuated and then immediately

filled by the liquid. After filling, a small amount of epoxy is used to seal the electrolyte injection channels. Figure 9 shows the liquid-filled chambers under fluorescence.

6. Test results

Deflection tests were first performed on the actuators by electrolysis (figure 10). The deflection is calibrated by an electromagnetic displacement sensor with a resolution of 0.02 μm. Figure 11 shows the maximum deflections the actuators can achieve by applying an electrolysis voltage of 5 V. Up to 100 μm of movement can be achieved by a 3 mm diaphragm. Experimental data show that the increasing rate of diaphragm deflection has a linear dependence on the electrolysis current. Figure 12 shows that the movement of the actuator can be linearly controlled by the current. Latchable and reversible movement are also demonstrated using the electrolysis actuators. Because hydrogen and oxygen are stored in two separated chambers, preventing recombination, figure 13 shows that the diaphragm can hold its position even with no power input. And when we reverse the voltage polarity, recombination happens in each chamber: the diaphragm goes backward then goes forward after recombination has finished. For example: in the central hydrogen chamber, after the voltage polarity is reversed, oxygen is generated in the chamber and meets the original hydrogen to recombine to water, resulting in backward movement of the membrane. After the hydrogen has totally recombined, more oxygen is generated in the chamber and the pressure increases again, therefore the membrane goes forward again. Figure 13 also shows several cycles of bidirectional movements. We observed that the membrane cannot return completely to its original position. This is because only the gas at the bottom of the chamber, which contacts the electrode, recombined. Some of the gases stay in the top of the chamber, because recombination occurs very slowly without a catalyst. Although the gases did not completely recombine in this experiment, recombination can be improved by adding a platinum catalyst to the electrolyte.

7. Conclusion and application

A large-force bidirectional electrolysis actuator has been fabricated with MEMS technology. Up to 100 μm of movement was achieved by a 3 mm diaphragm. With the power to penetrate brain tissue, high density, low power, bidirectionality and latchabilty (without power), the actuator has promising aspects for use as an electrolysis-based movable neural probe.

Acknowledgments

We wish to acknowledge the support of the National Institutes of Health and thank Mr Trevor Roper for assistance with fabrication.

References

Andersen R A *et al* 2004 Recording advances for neural prosthetics *Proc. 26th Annual Int. Conf. of the IEEE EMBS (San Francisco, CA, USA)*

Cameron C G and Freund M S 2002 Electrolytic actuators: alternative, high-performance, material-based devices *Proc. Natl Acad. Sci.* **99** 7827–31

Pan C-T, Yang A H, Shen A S-C, Chou A M-C and Chou A H-P 2002 A low-temperature wafer bonding technique using patternable materials *J. Micromech. Microeng.* **12** 611–5

Xie J, Miao Y, Shih J, He Q, Liu J, Tai Y-C and Lee T D 2004 An electrochemical pumping system for on-chip gradient generation *Anal. Chem.* **76** 3756–63